Revealing Invisible Prostate Cancer with VERDICT-MRI

Marta Masramon[1], Manju Mathew[2], Joey Clemente[2], Adam Retter[2], Natasha Thorley[2], Baris Kanber[1], Eoin Dineen[3], Greg Shaw[3,4,5], Veeru Kasivisvanathan[3], Martyn Carter[6], Aiman Haider[7], Alex Freeman[7], David Atkinson[2], Daniel C. Alexander[1], Shonit Punwani[2], and Eleftheria Panagiotaki[1]

[1]Hawkes Institute, University College London, London, United Kingdom, [2]Centre for Medical Imaging, University College London, London, United Kingdom, [3]Division of Surgery and Interventional Sciences, University College London, London, United Kingdom, [4]Department of Urology, UCLH, London, United Kingdom, [5]Department of Urology, Barts Health NHS Foundation Trust, London, United Kingdom, [6]Faculty of the Built Environment, University College London, London, United Kingdom, [7]Department of Pathology, UCLH, London, United Kingdom

Synopsis

Motivation: Prostate multi-parametric (mp)MRI misses 10-20% of PCa, presenting a need for enhanced imaging techniques.

Goal(s): To determine if VERDICT-MRI, when used alongside mpMRI, can improve the detection and characterization of mpMRI-invisible lesions.

Approach: We identify patients with mpMRI-invisible lesions from the Histo-MRI clinical trial (n=11). We use slice-to-slice matched whole-slide histology and MRI. We analyze differences in histological cell density, epithelial fraction and VERDICT intracellular volume fraction between mpMRI-visible and -invisible lesions.

Results: Using VERDICT-MRI improves the sensitivity of detection of invisible lesions, particularly with high cell density and epithelial fraction.

Impact: Integrating VERDICT-MRI into clinical imaging could enhance detection of previously invisible prostate cancer lesions, allowing for more precise stratification and more informed, personalized treatment strategies, potentially improving patient outcomes.

Introduction

The Prostate Imaging Reporting and Data System (PI-RADS) was developed to standardize acquisition, interpretation and reporting of prostate multi-parametric (mp)MRI examinations. It suggests staging of suspicious lesions based on T2W MRI, diffusion-weighted (DW) MRI, dynamic contrast enhancement and apparent diffusion coefficient (ADC) maps and has distinct guidelines for lesions in peripheral and transition zones (PZ, TZ)[1].

However, mpMRI can miss 10-20% of prostate cancer (PCa) lesions[2]. These invisible lesions have been associated with Black race and high PSA density[3]. Histologically, they tend to be smaller, with more heterogeneous morphology, and have lower Gleason Scores, cell density and epithelial fraction than visible lesions[4,5].

The fractional intracellular volume (fIC) from the Vascular, Extracellular, and Restricted Diffusion for Cytometry in Tumors (VERDICT) framework has demonstrated potential as an imaging biomarker when combined with mpMRI, offering greater accuracy in detecting clinically significant PCa than ADC maps, and enhancing the identification of false-positive lesions[6–9]. fIC has also been shown to correlate with histological cell density and epithelial fraction[10].

This study investigates the potential of VERDICT-MRI to aid in the detection of invisible lesions when used alongside mpMRI. We hypothesize that the incorporation of VERDICT-MRI will improve characterization of ambiguous lesions. For example, the pre-established fIC threshold for detection of clinically significant PCa (median fIC ≥ 0.41)[7] could enhance detection of invisible lesions with high cell density and epithelial fraction.

Methods

Patient data. We analyzed data from the Histo-MRI clinical trial (NCT04792138), where men with histologically confirmed PCa that are awaiting prostatectomy are scanned using clinical mpMRI and VERDICT-MRI[11] (n=48). 3D printed molds from pre-operative T2W MRI ensured slice-to-slice correspondence between MRI and histology. The specimen handling protocol is described in[12].

Comparing radiological reports from the initial clinical mpMRI against histological reports from whole-slide imaging (WSI), cases with invisible lesions on mpMRI were identified (n=11). These showed tumour foci on histological assessment that was not identified on the pre-surgical mpMRI. All undetected foci had Gleason score (GS) ≥ 3+4 and ranged in size from 0.6 to 104mm^2.

Histological analysis. Histologists segmented and graded lesions on WSI (454nm/pixel resolution). Histological parameter maps were obtained in a patch-based manner: cell density was derived from nuclei segmentations on QuPath[13], while tissue fractions (stroma, lumen, epithelium) were segmented semiautomatically with Image Pro (Media Cybernetics)[14].

VERDICT fitting. VERDICT parameter maps were obtained using multilayer perceptron fitting[9].

Statistical analysis. Differences between visible and invisible lesions across all parameter maps were analyzed by calculating the median value for each region of interest. Inter-group differences were represented by the mean difference and corresponding limits of agreement[15].

Results

Figure 1 shows an example of the histologically derived parameter maps and displays the differences in histological measures of cell density and epithelial fraction, as well as fIC, for mpMRI-detected and -invisible lesions. There are no statistically significant differences (Table 1) but, in all cases, the median value is higher for visible lesions.

Figure 2 shows example cases where the invisible lesions have median fIC above the defined threshold of 0.41. All cases shown have invisible lesions of GS 3+4 of varying sizes and, guided by the high-resolution T2W, can be clearly delineated on the VERDICT fIC map.

Figure 3 shows example cases where the invisible lesions have median fIC below the defined threshold. The invisible lesions all have GS 3+4 and cannot be seen on the T2W or VERDICT-MRI maps. Figure 4 shows that, in these cases, lesion are small and have low histological cell density and epithelial fraction.

Discussion and Conclusion

We show that invisible lesions tend to have lower fIC than detected lesions and corroborate previous findings that demonstrated reduced histological cell density and epithelial fraction in the latter. We find no statistical significance in the results, probably due to small sample size.

We illustrate various examples, cases where the fIC threshold could have been used to detect the invisible lesions and cases where it could not. We show that using the pre-established fIC threshold for detection of clinically significant PCa could allow the identification of invisible lesions and, in some cases, upgrade of lesions with low Likert score – considered clinically insignificant – into higher scores that require follow-up biopsy.

Overall, we show that the use of VERDICT-MRI alongside mpMRI in the staging of lesions could reduce the amount of missed PCa on MRI. Especially in cases where there is some indication of lesion but analysis of mpMRI is indeterminate, using fIC maps from VERDICT-MRI could aid in the detection of clinically significant PCa. Further work will investigate the effect of including VERDICT-MRI on specificity.

Acknowledgements

This work is supported by the EPSRC-funded UCL Centre for Doctoral Training in Intelligent, Integrated Imaging inHealthcare (i4health) [EP/S021930/1]; EPSRC grant numbers EP/N021967/1, EP/R006032/1; Prostate Cancer UK, TargetedCall 2014, Translational Research St.2, grant number PG14-018-TR2; the National Institute for Health and Care Research,University College London Hospitals Biomedical Research Centre; and Cancer Research UK National Cancer ImagingTranslational Accelerator.

References

1. Steiger, P. & Thoeny, H. C. Prostate MRI based on PI-RADS version 2: How we review and report. Cancer Imaging vol. 16 Preprint at https://doi.org/10.1186/s40644-016-0068-2 (2016).
2. Zhao, Y. et al. Comparison of Multiparametric Magnetic Resonance Imaging with Prostate-Specific Membrane Antigen Positron-Emission Tomography Imaging in Primary Prostate Cancer Diagnosis: A Systematic Review and Meta-Analysis. Cancers (Basel) 14, 3497 (2022).
3. Kuhlmann, P. K. et al. Patient- and tumor-level risk factors for MRI-invisible prostate cancer. Prostate Cancer Prostatic Dis 24, 794–801 (2021).
4. Chatterjee, A. et al. Prostate Cancers Invisible on Multiparametric MRI: Pathologic Features in Correlation with Whole-Mount Prostatectomy. Cancers (Basel) 15, (2023).
5. van Houdt, P. J. et al. Histopathological Features of MRI-Invisible Regions of Prostate Cancer Lesions. Journal of Magnetic Resonance Imaging 51, 1235–1246 (2020).
6. Johnston, E. W. et al. VERDICT MRI for prostate cancer: Intracellular volume fraction versus apparent diffusion coefficient. Radiology 291, 391–397 (2019).
7. Singh, S. et al. Avoiding Unnecessary Biopsy after Multiparametric Prostate MRI with VERDICT Analysis: The INNOVATE Study. Radiology (2022) doi:10.1148/radiol.212536.
8. Appayya, M. B. et al. The Intracellular Component of VERDICT (Vascular, Extracellular, and Restricted Diffusion for Cytometry in Tumors) MRI Distinguishes Gleason 4 Pattern Better than Apparent Diffusion Coefficient. (2018).
9. Sen, S. et al. Differentiating False Positive Lesions from Clinically Significant Cancer and Normal Prostate Tissue Using VERDICT MRI and Other Diffusion Models. Diagnostics 12, (2022).
10. Masramon, M. et al. Validation Of In Vivo VERDICT FIC Against Matched Histology From Whole-Mount Prostatectomy. in International Society for Magnetic Resonance in Medicine (ISMRM) (2024).
11. Singh, S. et al. Histo-MRI map study protocol: a prospective cohort study mapping MRI to histology for biomarker validation and prediction of prostate cancer. BMJ Open 12, e059847 (2022).
12. Bourne, R. M. et al. Apparatus for histological validation of in vivo and ex vivo magnetic resonance imaging of the human prostate. Front Oncol 7, (2017).
13. Bankhead, P. et al. QuPath: Open source software for digital pathology image analysis. Sci Rep 7, (2017).
14. Media Cybernetics. Image-Pro. https://mediacy.com/image-pro/.
15. Bland, J. M. & Altman, D. G. Measurement STATISTICAL METHODS FOR ASSESSING AGREEMENT BETWEEN TWO METHODS OF CLINICAL MEASUREMENT.

Figures

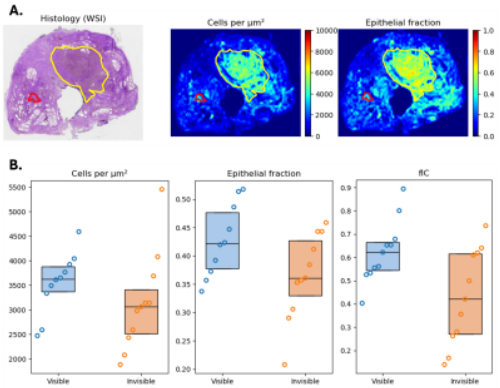

Figure 1. A. Example histology whole-slide image (WSI) with corresponding quantitative maps of derived cell density and epithelial fraction. **B.** Boxplots showing differences in histological features and fIC between mpMRI-visible and -invisible lesions.

	Visible *mean ± std. dev.*	**Invisible** *mean ± std. dev.*	*mean difference [95% CI]*
Cell density (per µm²)	3550 ± 605	3140 ± 957	408 [-332, 1148]
Epithelial fraction	0.43 ± 0.06	0.37 ± 0.07	0.06 [$3{\cdot}10^{-4}$, 0.12]
fIC	0.63 ± 0.13	0.43 ± 0.20	0.20 [0.05, 0.34]

Table 1. Analysis of histological parameters and VERDICT fIC in mpMRI-visible and -invisible lesions. Statistical significance represented by mean difference and corresponding 95% confidence intervals (CI).

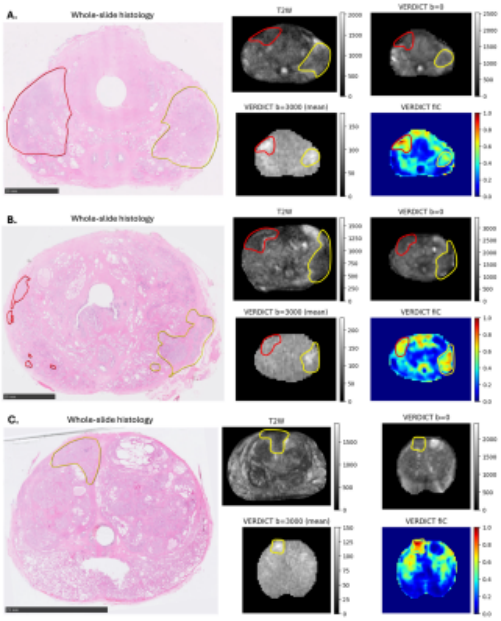

Figure 2. Examples where median fIC of invisible lesions is above threshold. Invisible lesions are outlined in red, reported lesions in yellow. **A**. Reported lesion in left posterolateral base of PZ (Likert 4, GS 3+4). Non-reported GS 3+4 lesion on the right, visible on VERDICT-MRI. **B.** Reported lesion in left posterolateral apex to base of PZ with some extension into left TZ (Likert 5, GS 4+3 with perineural invasion). Non-reported GS 3+4 lesions on the right, visible on VERDICT-MRI. **C.** Reported lesion in right TZ (Likert 2, GS 3+4). Could have been upgraded to higher Likert with VERDICT-MRI.

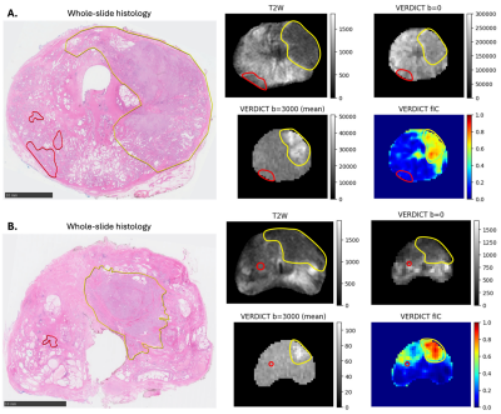

Figure 3. Examples where median fIC of invisible lesions is below threshold. Invisible lesions are outlined in red, reported lesions in yellow. **A.** Reported lesion in left apex (Likert 5, 3+4 with tertiary pattern 5 (<5%)). Non-reported GS 3+4 lesions on the right, invisible on VERDICT-MRI. **B.** Reported lesion in left PZ (Likert 4, GS 4+3). Non-reported GS 3+4 lesion on the right, invisible on VERDICT-MRI.

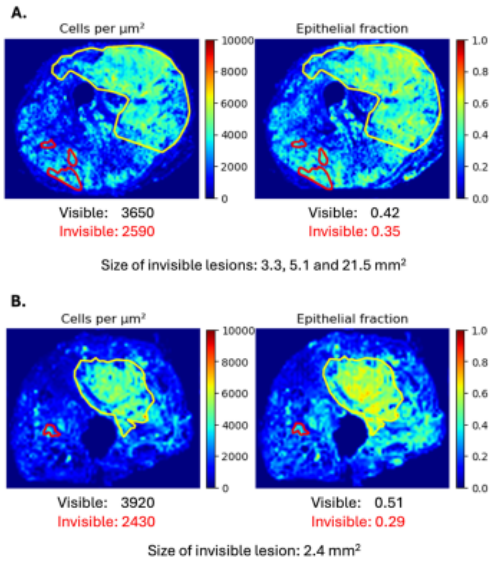

Figure 4. Exploration of histological features in cases where the invisible lesions are not detectable using mpMRI and VERDICT-MRI. Median values for the visible and invisible lesions are reported under each parameter map.